

Porous Epoxy Thermosets Obtained by a Polymerization-Induced Phase Separation Process of a Degradable Thermoplastic Polymer

Antonio García Loera, Fabien Cara, Michel Dumon,* and Jean Pierre Pascault

Laboratoire des Matériaux Macromoléculaires, CNRS UMR no. 5627, Institut National des Sciences Appliquées de Lyon; 20, Avenue Albert Einstein, F-69621 Villeurbanne Cedex, France

Received September 4, 2001; Revised Manuscript Received April 25, 2002

ABSTRACT: A process for producing controlled porous epoxy thermosets is presented. It is based on a two-step temperature cure: a polymerization-induced phase separation at a moderate temperature (100–120 °C) of a thermoplastic, poly(vinyl methyl ether) (PVME), in an epoxy–amine matrix followed by a high-temperature treatment (above 200 °C). A porous structure is created by the oxidative thermal degradation of PVME (extraction). Different porous or semiporous structures with submicrometer-sized voids (dispersed closed cells, i.e., spheres or open cells, i.e., bicontinuous percolating canals) are generated depending on the thermoplastic content and the phase-separation mechanism. The morphologies are analyzed quantitatively from transmission electron microscopy (TEM) photographs.

Introduction

Thermoset-based polymer blends often results from a polymerization-induced phase-separation method.¹ This method can also be used to prepare porous thermosetting polymers such as epoxy, cyanurate or dicyclopentadiene thermosets.^{2–6} In these cases, an organic solvent (a low molar mass liquid) is mixed with the monomer(s); the liquid is initially miscible in the monomers but separates upon polymerization. The morphology of the separated solvent droplets is fixed after gelation of the polymer matrix. Finally a porous polymer matrix is provided when the solvent is evaporated. Some applications of porous thermosets have been quoted: for example, high- T_g thermoplastics^{7,8} or thermosets⁹ were prepared for low permittivity films in microelectronics. They could also serve as matrix to host a second phase having functional properties such as conductive or electrooptical properties.

In this paper, we present porous thermosets prepared from the phase separation of a thermoplastic polymer and its consequent thermal degradation providing pores with either a submicrometer-sized closed-cell structure or a bicontinuous percolating structure (“canallike”) in an epoxy–amine cross-linked matrix.

When step-growth polymerization is used to induce phase separation, low-molar mass liquids hardly allow one to obtain bicontinuous structures because such a type of structure is usually reached in the vicinity of the critical point in a pseudobinary phase diagram.^{1,10} If the separating phase is a low molar mass molecule, the critical point lies at fairly high concentrations (e.g., >50 vol %).¹⁰ At such concentrations, macrophase separation often prevails over microphase separation. Also, due to their low viscosity compared to that of the reacting oligomers, low molar mass additives have the disadvantage to generate morphologies subject to coalescence, which may not be stable with time.

On the other hand, the use of high molar mass additives enables one to reach the vicinity of the critical point at concentrations between 10 and 30 vol % of additive.^{10,11}

In this paper, we have used a polymer additive (poly(vinyl methyl ether), PVME) which is likely to generate both closed-cell (i.e., nodules) and bicontinuous (i.e., “canals”) morphologies.

In the final step of the process, PVME is subjected to a thermal oxidative decomposition. Burns and Prime^{12,13} published a thermoset formulation for magnetic memory disk microporous coatings containing an epoxy–phenolic binder, magnetic particles, alumina, and PVME as a porosity forming agent. Porosities help to retention of lubricant and enhance durability of the disk. These formulations are complex and their chemistry is difficult to understand because, at the temperatures used (above 200 °C), several chemical reactions take place concomitantly with phase separation and decomposition of PVME. The mineral particles and PVME also participate to the cross-linking of the epoxy–phenolic binder.^{12,13} We chose a simpler formulation comprising only of a reactive diepoxy, a diamine monomer and PVME at different concentrations. Two amines were selected so that the epoxy can be cross-linked with either one or a mixture of the two amines in order to vary the pore size. The contribution of the present paper is the analysis of the phase-separation/degradation process in model systems and of the resulting morphologies depending on the initial amount of PVME.

Experimental Section

Materials and Sample Preparation. In Table 1 are given the chemical formulas and characteristics of the monomers and PVME used in this work. Poly(vinyl methyl ether) (PVME) is received as a water solution and is dried (12 h at 80 °C under vacuum) prior to mixing with DGEBA. Drying of PVME is checked by the disappearance of the OH water band in a FTIR spectrum. Then PVME–DGEBA solutions are prepared at 100 °C in a small reactor with a classical mechanical stirring for a few minutes. The amine(s) is (are) added and stirred for another 2 min in order to obtain a clear transparent solution. The solution (typically 3 g) is poured into a glass tube (height 7 cm, diameter 0.9 cm), closed by a cork. The reaction is carried out in the glass tube for 2 h at 100 °C. The epoxy–amine reaction kinetics is measured and described elsewhere.^{14,15} The ratio of amino hydrogen (N–H) to epoxy functions is equal to 1.

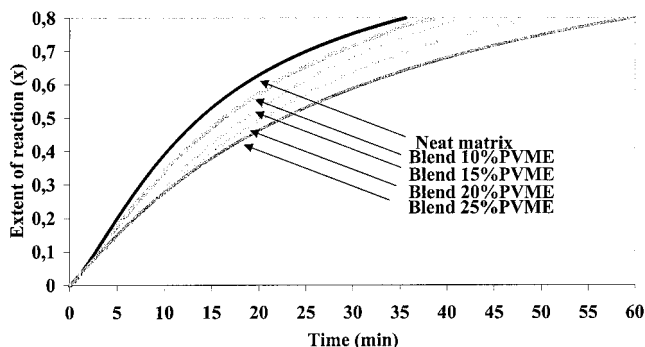
After polymerization, the glass tubes are broken and the samples are cut into specimens on which thermal degradation

* To whom correspondence should be sent.

Table 2. Some Characteristics of Polymerization and Properties of Cured Neat Matrices and Blends^a

neat matrix	ΔH^{react} (kJ/ee)	$x_{\text{gel}}^{\text{exp}}$	$x_{\text{gel}}^{\text{theo}}$	T_{g} (°C)	
DGEBA-D400	95 ± 4	0.58 ± 0.02	0.577	38	
DGEBA-T403	101 ± 4	0.49 ± 0.02	0.480	84	
DGEBA-D400 50 wt %–T403 50 wt %	95 ± 4			59	
blends	ΔH^{react}	$x_{\text{gel}}^{\text{exp}}$	$x_{\text{CP}}^{\text{exp}}$	T_{g}^{α}	T_{g}^{β}
DGEBA-T403/15 wt % PVME	100 ± 4	0.54 ± 0.02	0.44	81	–24
DGEBA-T403/20 wt % PVME	103 ± 4	0.54 ± 0.02	0.44	81	–25
DGEBA-T403/25 wt % PVME	102 ± 4	0.55 ± 0.02	0.45	81	–26
DGEBA-T403/30 wt % PVME	101 ± 4	0.54 ± 0.02	0.45	80	–25

^a ΔH^{react} is the epoxy-amine reaction enthalpy per epoxy equivalent. $x_{\text{gel}}^{\text{exp}}$ and $x_{\text{gel}}^{\text{theo}}$ are respectively the measured (by appearance of an insoluble fraction in THF) and calculated (by Macosko-Miller theory) gel point conversions. $x_{\text{CP}}^{\text{exp}}$ is the cloud point conversion measured by the appearance of turbidity at 100 °C. T_g is the glass transition temperature of fully cured matrices (taken at the midpoint on DSC thermograms); T_g^{α} and T_g^{β} are, respectively, the glass transition temperatures of the epoxy-amine-rich and PVME-rich phases.

**Figure 1.** Evolution of the polymerization conversions in epoxy-amine neat matrix and epoxy-amine/PVME blends.

point times (appearance of turbidity). In the presence of PVME (i.e., a nonreactive additive), the kinetics slows down with increasing the PVME weight fraction due to the dilution effect of the epoxy groups.^{14,17} The apparent gel conversions measured in blends (Table 2) are higher than those of the corresponding neat matrix. If one considers that, after phase separation the measured conversion in blends is an overall measurement of both phases; the measured average gel conversion would be decreased compared to a calculated gel conversion¹⁷ in the epoxy-amine-rich phase, which is not the present case. However, the effect of increase in gel point conversion has already been mentioned in other systems based either on the same epoxy-amine¹⁴ or the same amine and another epoxy.¹⁸ It is caused by dilution favoring an increased probability of cyclization and intramolecular reactions possible with the flexible amines chosen. Another explanation to account for the increase in gel point conversion is the change in stoichiometry of the epoxy-amine phase after phase separation, giving a preferential partition of the monomers and oligomers.

PVME Miscibility in the Monomers and Cloud Points during Polymerization. PVME is miscible in the three monomer mixtures over the whole concentration range at any temperature. No temperature-induced phase separation of PVME in any of the monomer mixtures is observed in the temperature range –100 to +100 °C. DSC scans of the mixtures, performed at 5 or 20 °C/min, exhibit only one T_g corresponding to one phase and obeying the Fox relation. In fact, the systems only vitrify, and phase separation does not occur. Therefore, the monomer systems based on either amines behave similarly regarding initial miscibility of PVME.

However the monomer systems behave very differently upon polymerization. The D400-based matrix containing 15 wt % PVME does not separate at any temperature up to full polymerization ($x = 1$). The cured

Table 3. Weight Loss of Neat Compounds or Blends after 10 h at 210 °C (TGA Results)

	sample mass (mg)	sample surface (mm ²)	wt loss at 210 °C/tot. sample mass (%)
DGEBA-T403/20 wt % PVME	25.7	57.1	7.6
DGEBA-T403/20 wt % PVME	25.4	64.6	8.5
DGEBA-T403/20 wt % PVME	25.3	74.4	9.4
neat PVME	27.5	51.3	24.9
DGEBA-T403	20.3	52.2	4
DGEBA-T403/15 wt % PVME	18.9	52.1	6.6
DGEBA-T403/20 wt % PVME	19.2	52.6	7.1
DGEBA-T403/30 wt % PVME	19.7	52.3	10.8

mixture exhibits only one T_g ($T_g = 28$ °C) obeying the Fox relation and is revealed to be quite transparent and homogeneous down to 10 nm (the TEM micrographs show no separated phase).

On the contrary, in the T403-based matrix containing 15 wt % PVME, opacity appears at a cloud point conversion of $x_{\text{CP}} = 0.44$ at 100 °C. Table 2 indicates that the cloud point conversions do not vary to a large extent within the investigated PVME concentration range. This behavior is explained in more details and modeled in ref 15. One can also notice that the T_g 's of the two separated phases are nearly equal to those of the neat components (matrix and PVME), which is an argument to say that the phases are nearly pure.

The thermodynamic reason for the difference in miscibility behavior between the two amines is analyzed in another paper through measurements of surface tension evolution during the course of polymerization.¹⁵

PVME Degradation. After polymerization, porous structures were obtained by treating the blends at a temperature of 210 or 250 °C for 10 h. At 250 °C for 10 h, the epoxy-amine always shows a mass loss of around or more than 10 wt % (depending on sample size), which made us choose a treatment temperature of 210 °C in order to minimize degradation of the matrix and to favor degradation (extraction) of PVME only as much as possible. However it should be admitted that polyoxypropylene diamine cross-linker is intrinsically prone to oxidation, and the choice of this cross-linker should be changed.

In similarity with Burns et al.,^{12,13} we measured a weight loss of only 25 wt % of neat PVME (in air) after 2 h at 210 °C.

For a same mass of the 20 wt % blend, the weight loss at 210 °C of samples with different surfaces is measured by TGA and reported in Table 3. It can be seen that the loss depends on the sample surface.

The weight loss of other blends are also reported in Table 3. The blends treated at 210 °C for 10 h showed

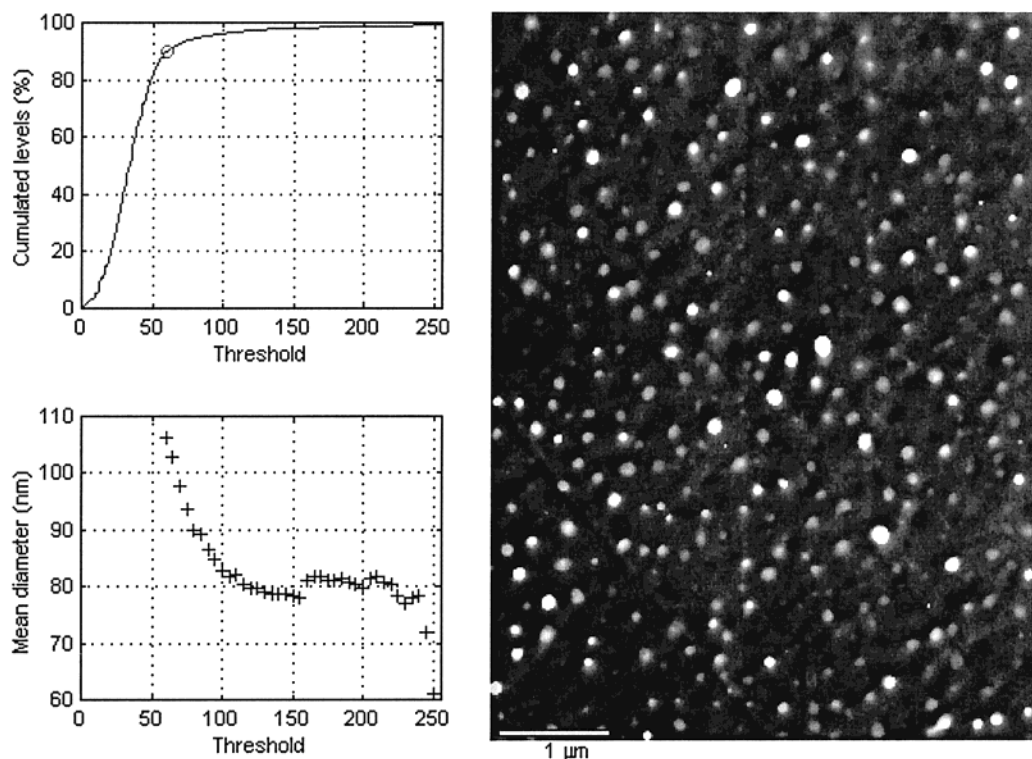


Figure 2. TEM photographs and analysis of the DGEBA-T403/10 wt % PVME blend.

a higher weight loss (Table 3) than PVME alone. Nevertheless, PVME is never completely extracted from the matrix at 210 °C, which is consistent with Burns' observations.

The previous authors mentioned that a maximum of 85 wt % of the introduced PVME is extractable from their particular epoxy binder after 4 h at 230 °C. These authors showed that PVME cannot be totally extracted because of oxidative self-cross-linking. The cross-linked products remain in the epoxy–phenolic matrix. They also mention that some reactions between PVME and the epoxy–phenolic matrix are even catalyzed by the presence of mineral oxidizing particles.

Indeed the degradation is an oxidative process that depends on the interfacial contact between air and the PVME phase. In a dispersed phase, the interfacial area is larger and thus PVME degrades better. However, once a cross-linked shell is formed, degradation is slowed.

Morphologies and Image Analysis of Blends after Degradation of PVME. Morphologies of porous (or semiporous) matrices initially containing 10, 15, 20, 25, or 30 wt % PVME have been observed by TEM after a thermal treatment of 10 h at 210 °C (see Experimental Section/Morphology).

Morphologies before thermal treatment show the same morphologies but with less contrast between phases. The neat matrix alone does not show any contrast before or after the thermal treatment.

Figures 2–5 show the experimental morphologies (as revealed by TEM) and two computed curves: the cumulated levels and the mean diameter vs threshold curves. In the composition range of PVME from 10 to 25 wt %, submicrometer sizes are always exhibited whatever the shape of voids. Such small sizes are stabilized thanks to the proximity between the cloud point and gel conversions.

To estimate the initial critical composition (before reaction), Φ_{crit} , we used eq 2 which is obtained from the Flory–Huggins model applied to a pseudobinary blend composed of a polydisperse thermoset and a polydisperse thermoplastic.¹

$$\Phi_{\text{crit}}^{-1} = 1 + (V_{\text{PVME}}/V_{\text{e-a}})^{0.5} [X_{\text{w(PVME)}}/(X_{\text{z(PVME)}})^{0.5}] \quad (2)$$

Equation 2 means that Φ_{crit} decreases with the square root of the additive molar mass.

V_{PVME} and $V_{\text{e-a}}$ are the molar volumes of the constitutional repeating unit of PVME and of the epoxy–amine pseudo component. $X_{\text{w(PVME)}}$ and $X_{\text{z(PVME)}}$ are the w and z average degrees of polymerization of PVME. They were calculated from the number-average molar mass measured by SEC ($M_n = 32\,000$) and a Schultz–Flory distribution;^{1,15} $X_{\text{w(PVME)}} \sim 1100$ and $X_{\text{z(PVME)}} \sim 1665$.

Thus, Φ_{crit} is estimated to be around 8–9%. Furthermore, it was shown that Φ_{crit} does not vary significantly with conversion and that the value of the initial (“unreacted”) critical point may be taken as a good estimate of the critical composition at the cloud point conversion.^{1,15}

Figures 2 and 3 show nodular or nearly nodular morphologies (10 and 15 wt % PVME) even. In the case of nodular morphologies, the image analysis indicates that the diameter–threshold level curve presents an asymptotic behavior to a size which accounts for the average diameter of pores: typically 70–80 nm for the 10 wt % blend and 150 nm for the 15 wt % blend. These PVME contents are therefore in the vicinity of the estimated critical region. The phase-separation process in epoxy–amine reactive systems of a high molar mass additive, between 10 and 30 vol %, has been demonstrated to be spinodal demixing.^{19,11} In the critical region, this phase-separation mechanism is likely to

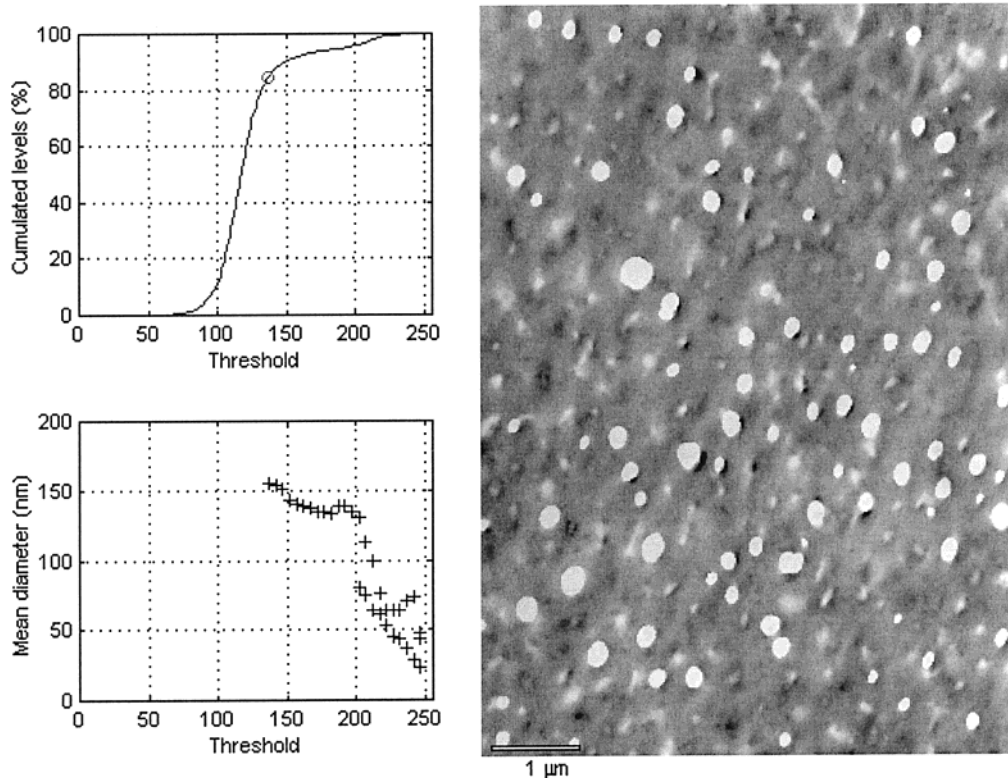


Figure 3. TEM photographs and analysis of the DGEBA-T403/15 wt % PVME blend.

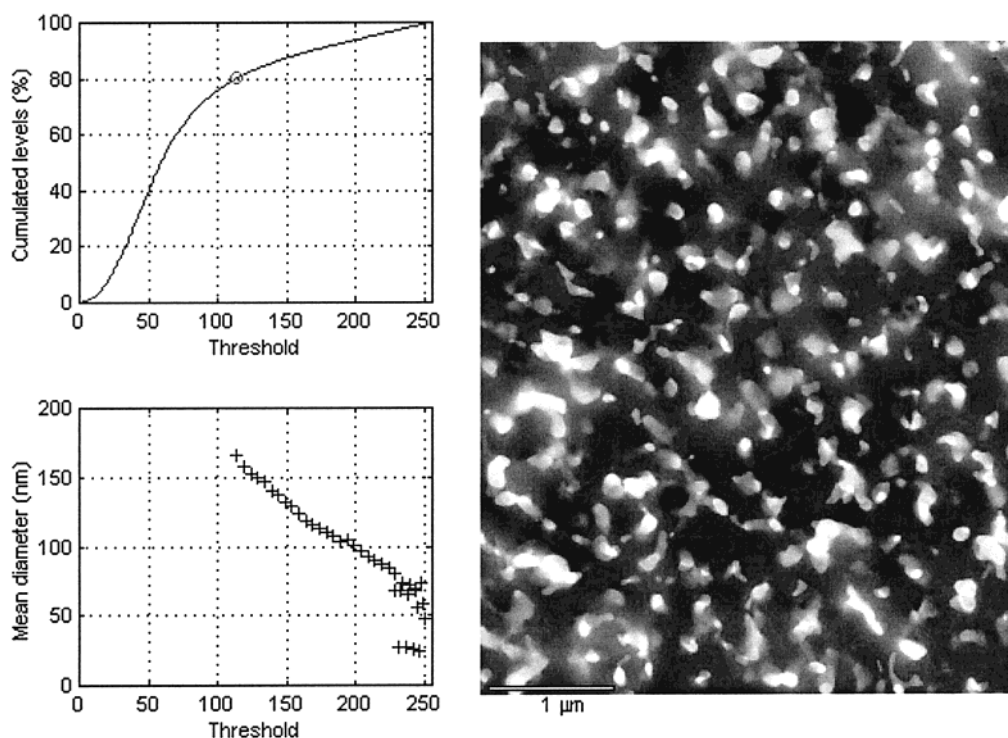


Figure 4. TEM photographs and analysis of the DGEBA-T403/20 wt % PVME blend.

exhibit morphologies with a high level of interconnectivity in both phases provided that the volume fraction of the separated phase is large enough to maintain a continuous separated phase. In our systems, at 10 and 15 wt % PVME contents, the thermoplastic rich domains cannot maintain the initial macroscopic percolation even if the initial phase-separation mechanism was spinodal demixing. One can observe that the voids tend to non spherical domains. Probably, the 15 wt % mass fraction

has nearly enough additive to begin to form a continuous thermoplastic phase.

As expected, the 20 wt % PVME blend (Figure 4) no longer presents a nodular morphology but exhibits elongated interconnected domains with no defined shapes. Indeed, the 20 wt % blend is within the critical region providing bicontinuous interconnected structures, and the weight fraction of PVME is high enough to maintain a final thermoplastic continuous phase. The

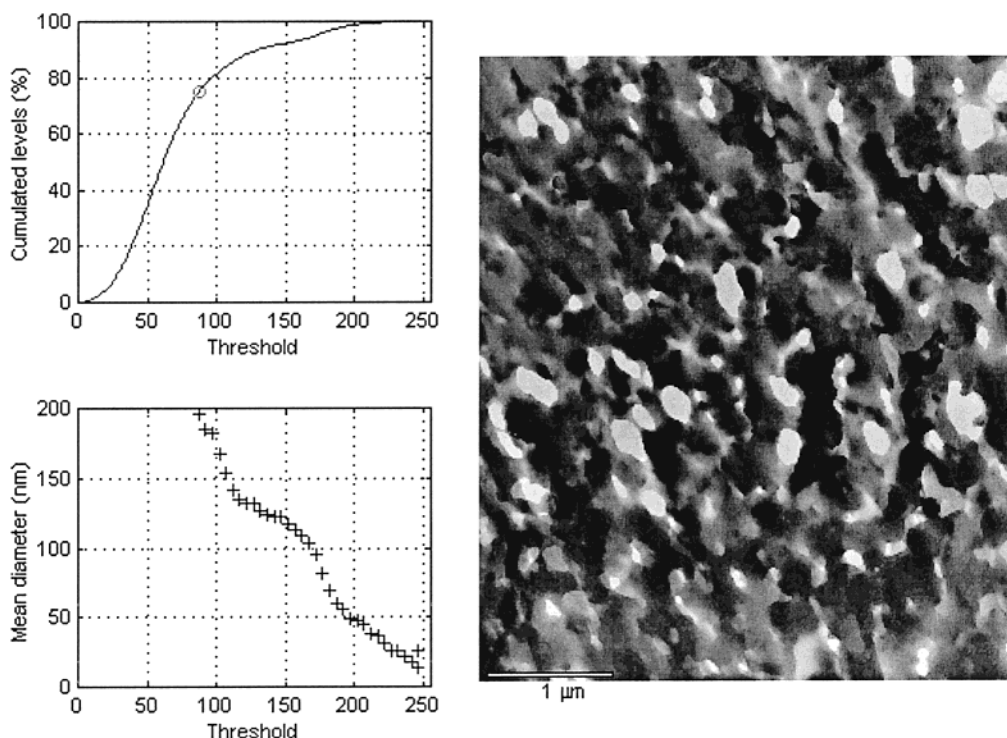


Figure 5. TEM photograph and analysis of the DGEBA-T403/25 wt % PVME blend.

observed morphologies (revealed by TEM) are the intersections of randomly oriented canals and the plane of the microtome cut (i.e., the observation plane). If a part of a canal *lies perpendicular* to the observation plane or if its size is of the order of the cut's thickness, the photograph shows a complete void. The TEM trace appears white (electrons are transmitted). If a part of the canal is *randomly oriented* compared to the observation plane or if its size is less than the sample cut's thickness, then the void is not crossing and the contrast on the TEM photograph appears gray. Furthermore, there may be superimposition of several canals within the thickness of a cut so that different gray levels appear on the TEM photograph. Another possibility (as already mentioned) is the incomplete degradation of PVME, giving uncomplete voids.

In contrast to nodular morphology, the diameter vs threshold level curve presents a monotonic decrease attesting that the separated domains have no definite, distinguishable size. Nevertheless, we can estimate an average dimension of domains assimilated to disks. Typical sizes range from 50 to 150 nm.

Finally, other experimental evidence can be put forward to say that the canals are interconnected: (a) during preparation of sample cuts of the 20 and 25 wt % blends, it was observed that water very rapidly swells the sample; (b) confocal microscopy, although only detecting the largest porous domains ($>1\ \mu\text{m}$), indicates that the canals situated in different observation planes, distant from several micrometers, communicate with each other.

The morphology of the 25 wt % PVME blend (Figure 5) is less clear because of difficulties to obtain thin TEM cuts (thin films are brittle at such void content). One can observe very bright areas that correspond to tearing of the matrix. However, Figure 5 again suggests an interconnected morphology. The 25 wt % blend is still in the critical region. The separated domains are larger than those of 20% blend due to a higher PVME content

and to possible coarsening. The typical size range lies from 25 to 200 nm.

At this point of the study, it is interesting to investigate morphologies obtained from a mixture of amines. The advantage of having two amines (one inducing phase separation and the other one inducing miscibility) is the possibility to use amine formulations in order to generate a great variety of morphologies by varying the amines weight ratio, keeping the stoichiometric ratio of amino hydrogen (N–H) to epoxy functions equal to 1.

One could expect that the matrix composed of a mixture of amines to give a morphology with smaller size. Indeed this is what is seen in a 20 wt % PVME blend with a matrix composed of 50/50 wt % of D400/T403. The pore size is decreased to around 40–50 nm.

Conclusion

Epoxy–amine thermoset/thermoplastic blends, precursors of porous polymer matrices, were prepared from initially homogeneous solutions of thermoset precursors and a thermoplastic, poly(vinyl methyl ether) (PVME). The process involves two steps: a polymerization induced phase separation of PVME followed by thermal degradation (extraction) of PVME at high temperature. PVME was confirmed to be only partially extractable by thermal degradation. According to the thermoplastic content, different morphologies with submicrometer-sized voids ($<200\ \text{nm}$) were stabilized: dispersed closed-cell or bicontinuous open-cell morphologies. The critical concentration was estimated to be around 10 wt % of thermoplastic. Even in the region of spinodal demixing, the observed final morphology may be spherical if too little thermoplastic is present (e.g., 10–15 wt %). From 20 to 25 wt % of thermoplastic, the morphologies are clearly bicontinuous.

The morphologies were analyzed quantitatively from TEM photographs by varying the threshold level on the

photograph from which the domains are considered as separated domains (complete or partial voids). By assimilation of the voids as spherical objects, diameter vs threshold level curves of nodular morphologies and of bicontinuous morphologies appear quite different (asymptotic behavior vs monotonic decrease).

References and Notes

- (1) Pascault, J. P.; Williams, R. J. J. In *Polymer Blends*; Paul, D. R., Bucknall, C. B., Eds.; Wiley Interscience: New York, 1999; Vol. 1, Chapter 13, pp 279–406.
- (2) Kiefer, J.; Hilborn, J. G.; Manson, J. A. E.; Leterrier, Y.; Hedrick, J. L. *Macromolecules* **1996**, *29*, 4158–4160.
- (3) Kiefer, J.; Porouchani, R.; Mendels, R.; Ferrer, J. B.; Fond, C.; Hedrick, J. L.; Kausch, H. H.; Hilborn, J. G. *MRS Symp. Proc.* **1996**, pp 527–532.
- (4) Kiefer, J.; Hilborn, J. G.; Hedrick, J. L. *Polymer* **1996**, *37*, 5715–5725.
- (5) Garcia Loera, A.; Dumon, M.; Pascault, J. P. *Macromol. Chem. Phys. Macromol. Symp.* **2000**, *151*, 341–346.
- (6) Della Martina, A.; Hilborn, J. G.; Muhlebach, A. *Macromolecules* **2000**, *33*, 2916–2921.
- (7) Hedrick, J. L.; Labadie, J.; Russell, T. P.; Wakharkar, V.; Hofer, D. *Mater. Res. Symp. Proc.* **1992**, Vol. 274, 37–45.
- (8) Hedrick, J. L.; Russell, T. P.; Labadie, J.; Lucas, M.; Swanson, S. *Polymer* **1995**, *36*, 2685–2697.
- (9) Kiefer, J.; Hilborn, J. G.; Hedrick, J. L.; Cha, H. J.; Yoon, D. Y.; Hedrick, J. C. *Macromolecules* **1996**, *29*, 8546–8548.
- (10) Williams, R. J. J.; Rozenberg, B. A.; Pascault, J. P. *Adv. Polym. Sci.* **1997**, *128*, 95–156.
- (11) Oyanguren, P. A.; Galente, M. J.; Andromaque, K.; Frontini, P. M.; Williams, R. J. J. *Polymer* **1999**, *40*, 5249–5255.
- (12) Burns, J. M.; Prime, R. B.; Barall, E. M.; Oxsen, M. E.; Wright, S. J. In *Polymers in information storage technologies, Symposium SEP*; 1988; pp 237–257; ISSN 0306433907.
- (13) *Thermal characterization of polymer materials*, 2nd ed.; Turi, A., Ed.; Academic press: New York, 1997; Vol 2, pp 1682–1696.
- (14) Masood Siddiqi, H.; Dumon, M.; Pascault, J. P. *Polymer* **1996**, *37*, 4795–4805.
- (15) Garcia Loera, A.; Dumon, M.; Pascault, J. P. Submitted for publication, 2001.
- (16) Miller, D. R.; Macosko, C. W. *Macromolecules* **1976**, *9*, 206–215.
- (17) Bonnet, A.; Pascault, J. P.; Sautereau, H.; Taha, M.; Camberlin, Y. *Macromolecules* **1999**, *32*, 8517–8523.
- (18) Dusek, K.; Ilavsky, M.; Stokrova, S.; Matejka, L.; Lunak, S. *Cross-linked epoxies*; Walter de Gruyter: Berlin, 1987; pp 279–289.
- (19) Girard Reydet, E.; Sautereau, H.; Pascault, J. P.; Keates, P.; Navard, P.; Thollet, G.; Vigier, G. *Polymer* **1998**, *39*, 2269–2278.

MA011567I